

# Long-range correlations and trends in Colombian seismic time series

L. A. Martín-Montoya<sup>a,c</sup>, N. M. Aranda-Camacho<sup>b,c</sup>, C. J. Quimbay<sup>c,d</sup>

<sup>a</sup>*Deutsches Elektronen-Synchrotron, Notkestr. 85, 22607 Hamburg, Germany*

<sup>b</sup>*University of São Paulo, Rua do Matão 1226, 05508-090, São Paulo, SP, Brazil*

<sup>c</sup>*Departamento de Física, Universidad Nacional de Colombia, Bogotá, D. C., Colombia*

<sup>d</sup>*Associate researcher of CIF, Bogotá, Colombia*

---

## Abstract

We detect long-range correlations and trends in time series extracted from the data of seismic events occurred since 1973 until 2011 in a rectangular region that contain mainly all the continental part of Colombia. The long-range correlations are detected by the calculation of the Hurst exponents for the time series of interevent intervals, separation distances, depth differences and magnitude differences. By using a geometrical modification of the classical  $R/S$  method that has been developed to detect long-range correlations in short time series, we find the existence of persistence for all the time series considered. We find also, by using the  $DFA$  until the third order, that the time series of interevent intervals, separation distances and depth differences are influenced by quadratic trends, while the time series of magnitude differences is influenced by a linear trend. Finally, for the time series of interevent intervals, we present an analysis of the Hurst exponent as a function of the time and the minimum number of windows.

---



---

*Email addresses:* `ligia.andrea.martin.montoya@desy.de` (L. A. Martín-Montoya), `nataly@iag.usp.br` (N. M. Aranda-Camacho), `cjquimbayh@unal.edu.co` (C. J. Quimbay)

## 1. Introduction

Among the properties that time series of different kinds phenomena exhibit, one of the most interesting is the long-range correlation [1]. This correlation, also known as long memory or long-range persistence, means that the autocovariance function decays exponentially, by a spectral density that tends to infinity [2, 3]. However, at the critical point, the exponential decay turns into a power-law decay [2, 4]. Long-range power-law correlations can be observed in a very wide range of systems, as for instance in smoke-particles aggregates [5], nucleotide sequences [6], earthquakes processes [7], mosaic structure of DNA [8], literary texts [9], stride interval of human gait [10], cardiac interbeat intervals [11], stock index variations [12], sedimentation [13], variations of daily maximum temperatures [14], neuron activity [15], stratus cloud liquid water [16], stock returns [3], electric signals [4], seismic sequences [17, 18], and relativistic nuclear collisions [19].

Long-range power-law correlations are traditionally measured by a scaling parameter or fractal dimension ( $D$ ). If the time series is self-similarity and self-affine, the parameter  $D$  is related with the Hurst exponent ( $H$ ) through the expression  $D = 2 - H$  [20, 21]. Thus, the Hurst exponent is a measure of the long-range correlation in time series data and allows to distinguish the persistence (correlation), anti-persistence (anti-correlation) or randomness of the data [22]. The original estimation of the Hurst exponent was first performed in hydrology by Harold Edwin Hurst in 1951 [23], by introducing an empirical relationship called the Rescaled-Range ( $R/S$ ). Posteriorly, this relationship became the start point to establish the Classical  $R/S$  ( $CR/S$ ) method developed by Mandelbrot and Wallis into the context of the fractal geometry [22, 24, 25].

Although the  $CR/S$  is one of the most popular methods to calculate the Hurst exponent, it has shown some serious limitations to study long-range correlation when the time series is not large enough [26]. However, a possible solution of this problem was proposed by Sánchez Granero *et al.* by means of a geometric method-based procedure, which we call the Geometric  $R/S$  ( $GR/S$ ) method [26, 27]. Another of the most popular methods to calculate the Hurst exponent is the Detrended Fluctuation Analysis ( $DFA$ ) proposed by Peng *et al.* [8]. One of the main advantages of the  $DFA$  is that it can remove trends present in some real time series [28, 29, 30]. Additionally, this method can be generalized for the multifractal characterization of nonstationary time series [31].

On the other hand, the study of long-range power-law correlations in seismic sequences has been focussed on the calculation of the Hurst exponent for times series of interevent intervals by using the *CR/S* [21] and the *DFA* [17, 18]. The *DFA* was also used to calculate the Hurst exponent associated to two-dimensional sequences defined in terms of the time series of interevent intervals and separation distances [32]. The Hurst exponents of time series of temporal and spatial variations were calculated using the *CR/S* method [33]. Starting from the values of the Hurst exponent calculated in these last references ( $0.5 < H < 1$ ), we enhance the existence of persistence for the temporal sequences [17, 18, 21, 33] and for the temporal-spatial sequences [32]. This result is consistent with the fractal structures in time, space, and magnitude dimensions observed in the seismicity of earthquakes [34, 35, 36]. However, most recently, it was observed an anticorrelated behavior ( $0 < H < 0.5$ ) of the earthquake magnitude time series from the calculation of the Hurst exponent using the *DFA* [37].

Until now the calculation of the Hurst exponent in seismic time series has been focussed in temporal, temporal-spatial and magnitude sequences [17, 18, 21, 32, 33, 37]. In this work we extend the detection of long-range correlations for the case of new time series that can be extracted from the seismic event data. Additionally to the time series of interevent intervals [17, 18, 21, 33, 39], we consider also the time series associated to the following parameters defined between two successive seismic events: separation distance [34, 32]; depth difference; magnitude difference. We think that if we study simultaneously the existence of long-range correlation for these four seismic time series, then we have a most complete vision of the fractal structure associated to the seismic events [34]. Because the interaction between a previous event and the event caused by it relaxes with the time, it is possible to observe simultaneously a self-similar structure in time, space and magnitude distributions of the seismic event epicenters [34, 35, 36].

The main goal of this work is to detect whether long-range correlations and trends exist in time series extracted from the data of seismic events occurred since 1973 until 2011 in a rectangular region that contain mainly all the continental part of Colombia. During this lapse of 39 years, the region under study, which contains also parts of Brazil, Ecuador, Panama, Peru and Venezuela, presented a total of 3932 seismic events with magnitudes higher than 4  $M_W$  according to the U.S. Geological Survey data base [38]. To detect the existence of long-range correlations in the time series of interevent intervals, separation distances, depth differences and magnitude differences,

we calculate the Hurst exponents associated to these time series by using the  $GR/S$  method [26, 27]. To appreciate the advantage of using the  $GR/S$  method, we first calculate the Hurst exponents for all the time series by using the  $CR/S$  method. With the purpose to eliminate trends in the seismic time series considered here, we calculate the Hurst exponents using the  $DFA$  until the third order [28, 29, 31].

The reason why we use the  $GR/S$  [26, 27] is because the  $CR/S$  might lead to an overestimation of the Hurst exponent, specially if seismic time series are constructed with less than 5000 data points as happened in this work. On the other hand, a study previously performed using data of Southern México [33] has detected the existence of cycles in the interevent interval sequence and this fact has been considered as a sign of trends in the associated seismic time series. For this reason in this work, we use also the  $DFA$  with the purpose to find polynomial trends on the data. We study also the evolution on time of the correlation between the Hurst exponent and the magnitude for the interevent interval in the seismological active area of the subduction zone of the Nazca and the South American plates in Colombia. The goal of this part of our study is to analyze if there is a statistical correlation between the value of the Hurst exponent and the magnitude of the seismic event, as it was found for the time series of interevent intervals in Southern México [33]. For accurateness, a study on the minimum number of windows in the calculation of the Hurst exponent is also performed, focussing the interest at the Hurst exponent as a function of the time and the minimum number of windows.

## 2. Methods to calculate the Hurst exponent

### 2.1. Classical Rescaled Range ( $CR/S$ )

The  $CR/S$  method allows to study the long-range dependence for non-stationary time series by means of the calculation of the Hurst exponent  $H$  [22, 24, 25]. Specifically, a value  $0 < H < 0.5$  corresponds to anticorrelated data (antipersistence behavior), a value  $0.5 < H < 1$  corresponds to correlated data (persistence behavior) and the value  $H = 0.5$  corresponds to random data (uncorrelated behavior) [22]. The definition of  $H$  can be extended for values larger than 1 [39]. In this form, the case  $H = 1.5$  corresponds to Brownian motion, the case  $H = 2$  correspond to brown noise and the case  $H > 2$  corresponds to black noise [39].

In the  $CR/S$  method the time series under consideration  $X : \{x_i\}$  is composed by  $N$  values. The full time series is divided into windows of size  $M$ . The number of windows is defined by  $s \equiv N/M$  and therefore there are  $s$  windows of data  $Y_j$ , with  $j = 1, 2, \dots, s$ .

Defining the vector  $k = (j-1)M + 1, (j-1)M + 2, (j-1)M + 3, \dots, (j-1)M + M$ , the average over each window is calculated as

$$\bar{y}_j = \frac{1}{M} \sum_k x_k. \quad (1)$$

The profile or sequence of partial summations  $Z_j : \{z_n\}$ , with  $n = 1, 2, \dots, M$ , is defined as the cumulative summation minus the average of the corresponding window

$$z_n = \sum_k^n \{x_k - \bar{y}_j\}. \quad (2)$$

The range  $R_j$  of the window is defined as the maximum minus the minimum data point of the profile

$$R_j \equiv \max\{Z_j\} - \min\{Z_j\}. \quad (3)$$

The standard deviation of each window  $\sigma_j$  is given as

$$\sigma_j = \left[ \frac{1}{M} \sum_k (x_k - \bar{y}_j)^2 \right]^{1/2}. \quad (4)$$

The rescaled range is described by the quantity  $(R/S)_s$ , which is defined as

$$(R/S)_s \equiv \frac{1}{s} \sum_j R_j / \sigma_j. \quad (5)$$

For the case in which a stochastic process associated to the data sequence under study is rescaled over a certain domain  $s \in \{s_{min}, s_{max}\}$ , the  $R/S$  statistics follows the power law

$$(R/S)_s = as^H. \quad (6)$$

Herein,  $a$  is a constant and  $H$  is the Hurst exponent which represents a fractal measure of the long-range correlations in the analyzed data.

## 2.2. Geometric Rescaled Range ( $GR/S$ )

When dealing with short time series (of less than 5000 values), the  $CR/S$  method loses precision [26]. Therefore, the inclusion of a correction factor, with a geometric interpretation that allows for a most precise calculation of

the Hurst exponent for the case of small data sets, results very convenient. This correction factor  $H_m$  was defined by Sánchez Granero *et al.* as [26, 27]

$$\log H_m \equiv \log(R/S)_m - \log E_m + \log(m)/2, \quad (7)$$

where  $E_m$  is

$$E_m \equiv \begin{cases} \frac{(m-\frac{1}{2})\Gamma(\frac{m-1}{2})}{m\sqrt{\pi}\Gamma(\frac{m}{2})} \sum_{i=1}^{m-1} \sqrt{\frac{m-i}{i}}, & \text{if } m \leq 340; \\ \frac{(m-\frac{1}{2})}{m\sqrt{m^{\frac{\pi}{2}}}} \sum_{i=1}^{m-1} \sqrt{\frac{m-i}{i}}, & \text{if } m \geq 340; \end{cases}$$

and  $m$  represents the minimum window size.

### 2.3. Detrended Fluctuation Analysis (DFA)

An important tool to leave out trends in time series is the *DFA* [28, 29, 30]. Trends can affect the time series and make them seem to be persistent when there is not a real correlation between the data points [28, 29, 30]. In the next, the method to calculate the Hurst exponent via *DFA* is explained.

As the first step of the *DFA*, it is necessary to calculate the profile or cumulative summations minus the average of all the data  $\bar{x}_i$

$$z_k = \sum_{i=1}^k x_i - \bar{x}_i, \quad (8)$$

where  $k$  runs over each data point  $k = 1, 2, 3, \dots, N$ .

As a second step, the profile is divided into  $s$  windows of size  $M$  and a fit of order  $l$  of the window is subtracted from each data point. Choosing the order to be  $l = 1$ , each new data point  $y_i$  is described as

$$y_k = z_k - \{a_j \cdot k - b_j\}, \quad (9)$$

where  $a_j$  and  $b_j$  are respectively the slope and the intercept of the linear fit done over the window  $j$ . For this case, the subscript  $j$  runs over the windows  $j = 1, 2, 3, \dots, s$ . The fluctuation is calculated as

$$F_M = \sqrt{\left[ \frac{1}{M} \sum_k y_k^2 \right]}. \quad (10)$$

Varying the size of the window  $M$  and consequently the number of windows  $s$ , the Hurst exponent  $H$  corresponds to the slope in the log-log plot of  $F_M$ .

If a stochastic process is associated to the data sequence under study, it will follow the power law

$$F_M = aM^H. \quad (11)$$

Different hierarchies of methods are employed for the fluctuation analysis. Those hierarchies differ from each other in how the fluctuations are measured and how trends are eliminated. By definition  $DFA_n$  eliminates trends of order  $n - 1$  in the original time series and  $n$  in the profile [28, 29, 30]. For instance,  $DFA_0$  corresponds to the simplest type of fluctuation analysis and in this case the trends are not eliminated. In the first order detrended fluctuation analysis  $DFA_1$ , the variance of the profile in each window represents the square of the fluctuations and then the best linear fit is determined [30].

### 3. Data acquisition

We consider in this work the time series associated to the following parameters defined between two successive seismic events: *(i)* interevent interval [17, 18, 21, 33, 39]; *(ii)* separation distance [34, 32]; *(iii)* depth difference; *(iv)* magnitude difference. We note that the seismic time series of depth differences and magnitude differences are new for this kind of analysis. Although this kind of analysis has been performed for time series of separation distance [32], the detection of long-range correlation for this time series that we present in this work is new in the literature because we consider the time series of separation distances as independent respect to the time series of interevent intervals. The time series of separation distance is extracted from the seismic event data using the following definition for the angular distance  $r$  in degrees between two events [34, 32]

$$r = \cos^{-1}[\cos(\theta_1) \cos(\theta_2) + \sin(\theta_1) \sin(\theta_2) \cos(\phi_1 - \phi_2)], \quad (12)$$

where  $(\theta_1, \theta_2)$  and  $(\phi_1, \phi_2)$  are respectively the colatitudes and the longitudes of the two events [34, 32]. If we multiply the the angular distance  $r$  by 111 km, then we obtain the separation distance between two suspensive seismic events [32].

The time series of interevent intervals, separation distances, depth differences and magnitude differences are constructed from the seismic event data that we have obtained from the free online database of the United States

Geological Survey [38]. A rectangular region that contains mainly all the continental area of Colombia was chosen to analyse the seismic data occurred since 1973 until 2011. As it is possible to observe in Figure 1, this region also contains parts of Brazil, Ecuador, Panama, Peru and Venezuela. Seismic events with magnitudes higher than 4  $M_W$  were selected in such a way that the total number of events initially considered was 3932. Using these data, Figure 2 presents the plot of the logarithm of the frequency as a function of the magnitude of the seismic event. The blue line in Figure 2 underlines the events with magnitudes from 4.8 to 6  $M_W$  that correspond to the ones that satisfy the Gutenberg-Richter law. Those events define the set that is used to perform the Hurst exponential analysis that will be presented bellow. It is important to mention that this methodology based in the Gutenberg-Richter law has been widely used in this kind of analysis [17, 18, 32, 21, 33].

#### 4. Persistence and trends in Colombian seismic data

Long-range correlations for temporal and temporal-spatial sequences have been detected previously by the calculation of Hurst exponent for different seismic active areas of the world, as for instance of Italy [17, 18], USA [32, 37, 39], Taiwan [21], México [33], and Greece [40]. In this section we present the results of the calculation of the Hurst exponent for the Colombian seismic time series of interevent intervals, separation distances, depth differences and magnitude differences. Firstly, we present the Hurst exponent that were calculated using both the  $CR/S$  and  $GR/S$  methods. By using the  $GR/S$  method, we obtain Hurst exponents most precise, correcting the effect of insufficiency of data (less than 5000 data points). Secondly, we present the Hurst exponents calculated using the  $DFA$  until the third order. In this way, we can remove the trends which are present in the seismic time series under study.

##### 4.1. Hurst exponents and the scarcity effects

A correct degree of long-range correlation, represented by a precise calculation of the Hurst exponent, in time series composed by a relative small quantity of data can not be possible to obtain by using the  $CR/S$  method. The  $CR/S$  method leads to an overestimation of the Hurst exponent for the considered seismic time series. This means that a fake degree of long-range correlation is originated by an insufficient number of data. This inaccuracy of the Hurst exponent calculated using the  $CR/S$  method for less than 5000



data points was proved for capital markets [26]. We find that if the four seismic time series are analysed using the  $GR/S$  method, then the Hurst exponents ( $H_G$ ) obtained with this geometric method are smaller than the ones calculated by the  $CR/S$  method ( $H_C$ ). We show in the Table 1 the differences between the Hurst exponents calculated using both methods, for the time series of interevent intervals, separation distances, depth differences and magnitude differences.

Time series	$H_C$	$H_G$
<i>Interevent intervals</i>	0.7875	0.6018
<i>Separation distances</i>	0.7761	0.6387
<i>Depth differences</i>	0.7273	0.6606
<i>Magnitude differences</i>	0.6747	0.6036

*Table 1.* Hurst exponent values calculated via the  $CR/S$  and the  $GR/S$  methods for the time series of interevent intervals, separation distances, depth differences and magnitude differences.

For the case of time series composed of around 2000 data points, as is the case of the four seismic time series analysed in this work (after filtering events that satisfy the Gutenberg-Richter law), a high level of long-range correlation on the data showed up though an overestimation of the Hurst exponents via the  $CR/S$  method. In other words, the scarcity of data points in the analysis misleads to a fictitious higher long-range correlation. The level of long-range correlation is still not the biggest concern as it is the accurateness of the method to establish if there is correlation or if randomness or anti-correlation govern the dynamics.

Although we have found an overestimation of the correlation level in the seismic time series using the  $CR/S$  method, *i.e.*  $H_C > H_G$ , still Hurst exponents above 0.5 are obtained by using the  $GR/S$  method. This is an important result of non-randomness for the main parameters of an seismic event, *i.e.* time, location and magnitude of seismic events, meaning they are not arbitrary and therefore a fractal structure describes their behavior. In this sense, non-randomness implies the presence of patterns behind the structure of the series and potentially a model of future events in terms of time, location and magnitude could be possibly proposed. Nevertheless, the inclusion of a such model is outside of the goals of this paper. Furthermore, the level of long-range correlation is proportional to the Hurst exponent and the trust values of  $H$  are obtained via the  $GR/S$  method. Values of the

$H_G$  shown in Table 1, indicate that the persistences associated to the time series of separation distances and depth differences are larger than the ones associated to the time series of interevent intervals and magnitude differences. Therefore, the location dynamics of the next seismic event are most persistent than the ones of time and magnitude.

#### 4.2. Hurst exponents and the hidden trends

Tectonic plate kinetics are not isolated but on the contrary they do coexist with numerous of other phenomena that are cyclic in time, *e.g.* seasons or tides. To inspect those aspects for seismic time series, we employ the DFA that makes possible to see whenever the data are affected by different orders of polynomial trends and with this implementation detrended Hurst exponent estimations are feasible.

The *DFA* has been used to study the existence of trends in financial time series (see [41] and references therein). In this section, we implement the *DFA* to study the existence of trends in seismic time series. This method allows removing trends of order  $n - 1$  in the data and the comparison between different  $n$  orders gives an evidence of specific polynomial order of trends. For the case in which the Hurst exponent calculated with  $DFA_{n+1}$  is smaller than the corresponding one with  $DFA_n$ , higher long-range correlations are in fact masked by the presence of trends of order  $n$ .

Following the analysis via the *DFA* until the third order, we obtain that the time series of interevent intervals, separation distances and depth differences present quadratic trends. We can make this conclusion starting from the Hurst exponents that we present in Table 2, due to the fact that  $H_{DFA_2}$  are greater than  $H_{DFA_3}$  for the case of these three time series. Furthermore, we observe that persistence is dominating the time series of interevent intervals, separation distances, and depth differences when the trends are excluded from the analysis (through Hurst exponents calculated via  $DFA_3$ ) with  $0.5 < H_{DFA_3} < 1$ .

Time series	$H_{DFA_1}$	$H_{DFA_2}$	$H_{DFA_3}$
<i>Interevent intervals</i>	0.7746	0.7907	0.7726
<i>Separation distances</i>	0.7871	0.7913	0.7836
<i>Depth differences</i>	0.7772	0.7921	0.7826
<i>Magnitude differences</i>	0.5396	0.5548	0.5556

Table 2. Hurst exponent values calculated using  $DFA_1$ ,  $DFA_2$  and  $DFA_3$  for the

times series of interevent intervals, separation distances, depth differences and magnitude differences.

Although trends in seismic time series account different physical origins and could be tricky to explain, Alvarez *et al.* have warned of one year cycles affecting interevent intervals for Southern México and suggested tidal effects influencing the dynamics of seismicity [33]. In the present work, we have examined the presence of possible polynomial trends of order one or two and we have found out that the expected cycles could be described as quadratic trends in the data. Since trends lead to an overestimation of the correlation level as well as the scarcity of data does, the progress here is not only the identification of the model of trends affecting interevent intervals but the removal of those trends from the analysis through the *DFA*. On the other hand, quadratic trends (possibly cyclic) do not affect only the time series of interevent intervals but the ones of separation distances and depth differences as well, while the time series of magnitude differences appears to have random fluctuations with a Hurst coefficient very close to 0.5.

The analysis of trends on the data allows to identify fake correlations on the time series of magnitude differences which seems to be persistent with the calculation of the Hurst exponent using the *GR/S* method. For this case, constant trends were making the magnitude's fluctuations as persistent while in fact randomness governs their origin.

## 5. Colombian subduction zone

The highest level of seismic activity in Colombia is due to the presence of subduction zones. Plate boundaries of Nazca, South American and Caribbean converge creating the most representative origin of seismic events in this area. Therefore, with the aim to give more insights about the nature of the seismic fluctuations, the area that encloses the subduction of the Nazca plate beneath the South American plate has been selected for the study that we present in this section, in order to account events with a common physical nature.

We inspect the behavior of the Hurst exponent when the minimum number of windows  $s_{min}$  is varied in the calculation, with the purpose to find the most suitable value of  $s_{min}$  that depends on the number of events considered in time.

In the second part of this section, we explore the agreement in the time evolution between the magnitude and the Hurst exponent on the seismic

time series. For this analysis three different minimum number of windows are chosen. Meaningful results for waiting times were reported previously for the Southern México [33]. We extend here these results for the case of time series of interevent intervals associated to the Colombian subduction zone.

### 5.1. Hurst exponent and the maximum window size

The dependence of the Hurst exponent with the maximum window size  $M_{max}$  has been widely studied for time series. However, it has been always difficult to establish criteria that determine the relationship between this parameter and the total number of data points. This dependence is extremely important for the study of the time evolution of the Hurst coefficient. Varying the maximum window size  $M_{max}$ , that is equivalent to vary the minimum number of windows  $s_{min}$  and taking a minimum window size of 5 events as a threshold for enough statistics, we obtain the behavior of the Hurst exponent associated to the seismic data from 1975 to 2011, that correspond from 100 to 340 events, for the  $CR/S$  and  $GR/S$  methods, as it is illustrated in Figure 3.

When comparing results from the  $CR/S$  method (Figure 3(a)) and the  $GR/S$  method (Figure 3(b)), it is possible to observe that there is an overall constant overestimation of the Hurst exponent calculated via the  $CR/S$  method of about 0.2. The scarcity of the seismic data points for the subduction in the years of study makes the use of the  $GR/S$  method as an ideal skill to calculate Hurst exponents.

Several features are found from the behavior of  $H$  as a function of time and  $s_{min}$  via the  $GR/S$  method (Figure 3(b)). First, long-range correlations seem to be higher if we take a smaller minimum number of windows. In this sense, for  $s_{min}$  smaller than 6, random dynamics describe the time series until the 200 event approximately. In general,  $H(t, s_{min})$  presents an error of  $\pm 0.1$  on the correlation level. This error depends on the time series under study as well as on the range of  $s_{min}$  and the time range selected.

### 5.2. Space relation between the Hurst exponent and the magnitude

We analyze only those events which follow the Gutenberg-Richter law, with magnitudes between 4.8 and 6  $M_W$ . We can observe in Figure 4(a) different areas of low magnitude that we call *low-magnitude gaps*. In a previous work [33], it was demonstrated that those low-magnitude gaps are closely related to low correlation level with values of  $H$  around 0.5. In the present work, we investigate this relation for the case of the time series of interevent

intervals. The results obtained show that  $H$  is closer to 0.5, for the *low-magnitude gap* between the 100 and the 175 event (see Figure 4(b)). For the case of the seismic events with magnitudes from 6 to 5.5  $M_W$ , the Hurst exponent becomes also closer to 0.5. This fact means a random behavior for low magnitude events.

In this work, the relationship obtained between the magnitude and the Hurst exponent can be considered as an extension of the one obtained in [33], but including several values of the minimum number of windows  $s_{min}$ . The results that we have obtained are shown in Figure 4(b), for three different minimum number of windows. The upper curve corresponds to  $s_{min} = 2$ , where a correspondence between the magnitude and the Hurst coefficient can not be established. The middle and the lower curves account  $s_{min}$  values of 4 and 7 respectively, and these curves show certain correlation in the behavior of the persistence evolution and the magnitude evolution. For both curves, there is a gap from 114 to 174 of low Hurst exponents closer to 0.5. Therefore, a relation between random behavior and low seismic activity is found for the Colombian subduction zone.

If we regard, for values higher than 2, the dependence of  $H$  respect to the  $s_{min}$ , then the behavior of the Hurst exponent is reproducing more accurately the evolution on time of the magnitude. This fact could be taken as a desirable threshold for the minimum number of windows on the  $R/S$  analysis, since  $s_{min} = 4$  as well as  $s_{min} = 7$  reproduce more accurately the magnitude dynamics than  $s_{min} = 2$ .

## 6. Conclusions

The seismic time series of interevent intervals, separation distances, depth differences, and magnitude differences are found to be persistent via the  $CR/S$  method. Nevertheless, using the  $GR/S$  method, it is determined that an overestimation on the Hurst exponent  $H$  affect all the series due to the scarcity of data points (around 2000). Despite the overestimation mentioned above, all the time series under consideration present persistence with  $0.5 < H_G < 1$ , when corrections via the  $GR/S$  method are taken into account.

Quadratic trends are detected via the comparison between different hierarchies of the  $DFA$  for the time series of interevent intervals, separation distances, and depth differences. In this sense, cyclic effects that were found in a previous work [33] could be explained as quadratic trends in the data.

On the other hand, the presence of constant trends makes the time series of relative magnitude to seem correlated when in fact  $DFA_1$  shows a Hurst exponent very close to 0.5 pointing out randomness.

For the time series of interevent intervals, the analysis of the Hurst exponent as a function of the time and the minimum number of windows has shown that  $s_{min} > 2$  is ideal for calculations, since it is describing better the dynamics of seismic events. Furthermore, we have found an agreement in the time evolution between low magnitude events and the value of Hurst exponent closer to 0.5 for the gap between 114 and 174 events.

## References

- [1] H. E. Stanley, *Introduction to phase transitions and critical phenomena*, Oxford University Press, London, 1971.
- [2] R. N. Mantegna, and H. E. Stanley, *An introduction to econophysics: Correlations and complexity in finance*, Cambridge University Press, Cambridge, 2000.
- [3] P. Grau-Carles, *Empirical evidence of long-range correlations in stock returns*, Physica A 287 (2000) 396-404 .
- [4] P. A. Varotsos, N. V. Sarlis, and E. S. Skordas, *Long-range correlations in the electric signals that precede rupture*, Phys. Rev. E 66 (2002) 011902.
- [5] S. R. Forrest, and T. A. Witten Jr., *Long-range correlations in smoke-particle aggregates*, J. Phys. A: Math. Gen. 12 (1979) L109-L117.
- [6] C. -K. Peng, S. V. Buldyrev, A. L. Goldberger, S. Havlin, F. Sciortino, M. Simons, and H. E. Stanley, *Long-range correlations in nucleotide sequences*, Nature 356 (1992) 168-170.
- [7] T. Hirabayashi, K. Ito, and T. Yoshii, *Multifractal analysis of earthquakes*, Pure Appl. Geophys. 138 (1992) 591-610.
- [8] C. -K. Peng, S. V. Buldyrev, S. Havlin, M. Simons, H. E. Stanley, and A. L. Goldberger, *Mosaic organization of DNA nucleotides*, Phys. Rev. E 49 (1994) 1685.

- [9] W. Ebeling, and T. Poschel, *Entropy and long range correlations in literary English*, Europhys. Lett. 26 (1994) 241-246.
- [10] J. F. Hausdorff, C. -K. Peng, Z. Ladin, J. Y. Wei, and A. L. Goldberger, *Is walking a random walk? Evidence for long-range correlations in stride interval of human gait*, J. of Appl. Physiol. 78 (1995) 349-358.
- [11] C. -K. Peng, S. Havlin, H. E. Stanley, and A. L. Goldberger, *Quantification of scaling exponents and crossover phenomena in nonstationary heartbeat time series*, Chaos 5 (1995) 82-87.
- [12] Y. Liu, P. Cizeau, M. Meyer, C. -K. Peng, and H. E. Stanley, *Correlations in economic time series*, Physica A 245 (1997) 437-440 .
- [13] P. N. Segre, E. Herbolzheimer, and P. M. Chaikin, *Long-range correlations in sedimentation*, Phys. Rev. Lett 79 (1997) 2574 .
- [14] E. Koscielny-Bunde, A. Bunde, S. Havlin, H. Eduardo Roman, Y. Goldreich, and H. J. Schellnhuber, *Indication of a universal persistence law governing atmospheric variability*, Phys. Rev. Lett. 81 (1998) 729-732.
- [15] S. Blesic, S. Milosevic, D. Stratimirovic, and M. Ljubisavljevic, *Detrended fluctuation analysis of time series of a firing fusimotor neuron*, Physica A 268 (1999) 275-282.
- [16] K. Ivanova, and M. Ausloos, *Application of the detrended fluctuation analysis (DFA) method for describing cloud breaking*, Physica A 274 (1999) 349-354.
- [17] L. Telesca, V. Lapenna, and M. Macchiato, *Mono- and multi-fractal investigation of scaling properties in temporal patterns of seismic sequences*, Chaos Sol. Frac. 19 (2004) 1-15.
- [18] L. Telesca, and M. Macchiato, *Time-scaling properties of the Umbria-Marche 1997-1998 seismic crisis, investigated by the detrended fluctuation analysis of interval time series*, Chaos Sol. Frac. 19 (2004) 377-385.
- [19] S. Gavin, L. McLerran, and G. Moschelli, *Long range correlations and the soft ridge in relativistic nuclear collisions*, Phys. Rev. C 79 (2009) 051902(R).

- [20] J. Feder, *Fractals*, Plenum Press, New York, 1988.
- [21] C. Chen, Y. Lee, and Y. Chang, *A relationship between Hurst exponents of slip and waiting time data of earthquakes*, Physica A 387 (2008) 4643-4648.
- [22] B. B. Mandelbrot, and J. R. Wallis, *Noah, Joseph and the operational hydrology*, Water Resour. Res. 4 (1968) 909-918.
- [23] H. E. Hurst, *Long-term storage capacity of reservoirs*, Trans. Am. Soc. Civil Eng. 116 (1951) 770-808.
- [24] B. B. Mandelbrot, and J. R. Wallis, *Some long-run properties of geophysical records*, Water Resour. Res. 5 (1969) 321-340.
- [25] B. B. Mandelbrot, and J. R. Wallis, *Robustness of the rescaled range  $R/S$  in the measurement of noncyclic long-run statistical dependence*, Water Resour. Res. 5 (1969) 967-988.
- [26] M. A. Sánchez Granero, J. E. Trinidad Segovia, and J. García Pérez, *Some comments on Hurst exponent and the long memory processes on capital markets*, Physica A 387 (2008) 5543-5551.
- [27] J. E. Trinidad Segovia, M. Fernández-Martínez, and M. A. Sánchez Granero, *A note on geometric method-based procedures to calculate the Hurst exponent*, Physica A 391 (2012) 2209-2214.
- [28] J. W. Kantelhardt, E. Koscielny-Bunde, H. H. Rego, S. Havlin, and A. Bunde, *Detecting long-range correlations with detrended fluctuation analysis*, Physica A 295 (2001) 441-454.
- [29] K. Hu, P. Ch. Ivanov, Z. Chen, P. Carpena, and H. E. Stanley, *Effect of trends on detrended fluctuation analysis*, Phys. Rev. E 64 (2001) 011114.
- [30] J. F. Eichner, E. Koscielny-Bunde, A. Bunde, S. Havlin, and H. - J. Schellnhuber, *Power-law persistence and trends in the atmosphere: A detailed study of long temperature records*, Phys. Rev. E 68 (2003) 046133.



- [31] J. W. Kantelhardt, S. A. Zschiegner, E. Koscielny-Bunde, S. Havlin, A. Bunde, and H. E. Stanley, *Multifractal detrended fluctuation analysis of nonstationary time series*, Physica A 316 (2002) 87-114.
- [32] L. Telesca, M. Lovallo, V. Lapenna, and M. Macchiato, *Long-range correlations in two-dimensional spatio-temporal seismic fluctuations*, Physica A 377 (2007) 279-284.
- [33] J. Alvarez-Ramirez, J. C. Echeverria, A. Ortiz-Cruz, and E. Hernandez, *Temporal and spatial variations of seismicity scaling behavior in Southern Mexico*, J. of Geodyn. 54 (2012) 1-12.
- [34] T. Hirata, *A correlation between the b value and the fractal dimension of earthquakes*, J. of Geophys. Res. 94 (1989) 7507-7514.
- [35] Z. Guo, and Y. Ogata, *Correlation between characteristic parameters of aftershock distributions in time, space and magnitude*, Geophys. Res. Lett. 22 (1995) 993-996.
- [36] Z. Guo, and Y. Ogata, *Statistical relations between the parameters of aftershock distributions in time, space and magnitude*, J. of Geophys. Res. 102 (1997) 2857-2873.
- [37] P. A. Varotsos, N. V. Sarlis, and E. S. Skordas, *Scale-specific order parameter fluctuations of seismicity before mainshocks: Natural time and detrended fluctuation analysis*, EPL 99 (2012) 59001.
- [38] U.S. Geological Survey, Earthquake data base, USGS, accessed [Oct. 31, 2011] at URL [<http://earthquake.usgs.gov/earthquakes/search/>].
- [39] A. Jimenez, *Comparison of the Hurst and DEA exponents between the catalogue and its clusters: The California case*, Physica A 390 (2011) 2146-2154.
- [40] Y. Xu, and P. W. Burton, *Time varying seismicity in Greece: Hurst's analysis and Monte Carlo simulation applied to a new earthquake catalogue for Greece*, Tectonophysics 423 (2006) 125-136.
- [41] K. Domino, *The use of the Hurst exponent to predict changes in trends on the Warsaw Stock Exchange*, Physica A 390 (2011) 98-109.

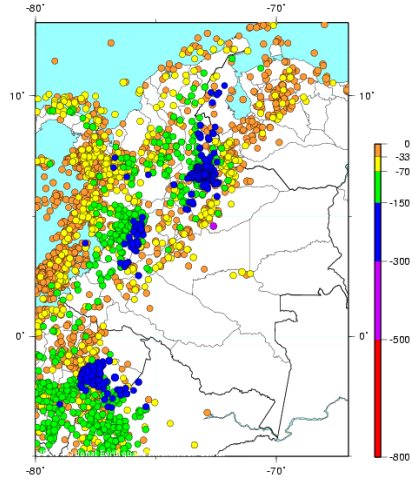


Figure 1: Selected region for analysis of seismic data. Events occurred since 1973 until 2011 are shown as small circles with different colors accordingly with the depth of the event [38].

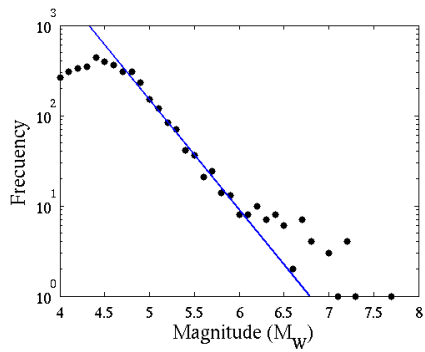


Figure 2: Logarithm of frequency vs. magnitude for the seismic events occurred since 1971 until 2011 in the selected region. The blue line shows the events that satisfy the Gutenberg-Richter law. Only events from 4.8 to 6  $M_W$  were used to perform the Hurst exponential analysis.

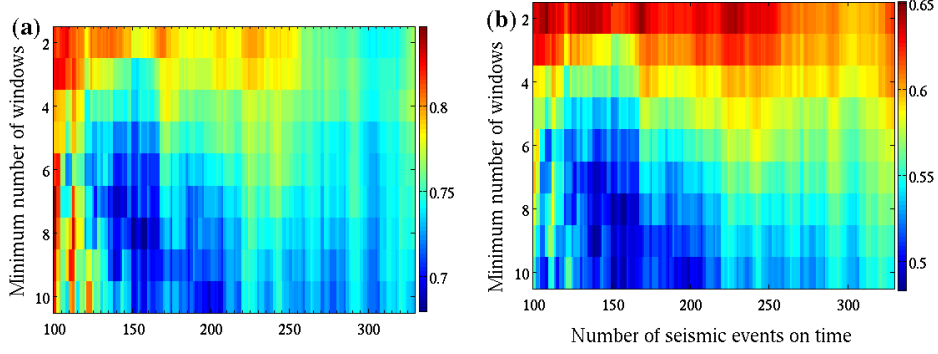


Figure 3: Behavior of the Hurst exponent under the variation of the minimum number of windows (maximum window size) and total number of events considered in time. **(a)** Hurst exponent calculated with the *CR/S* method. **(b)** Hurst exponent calculated using the *GR/S* method.

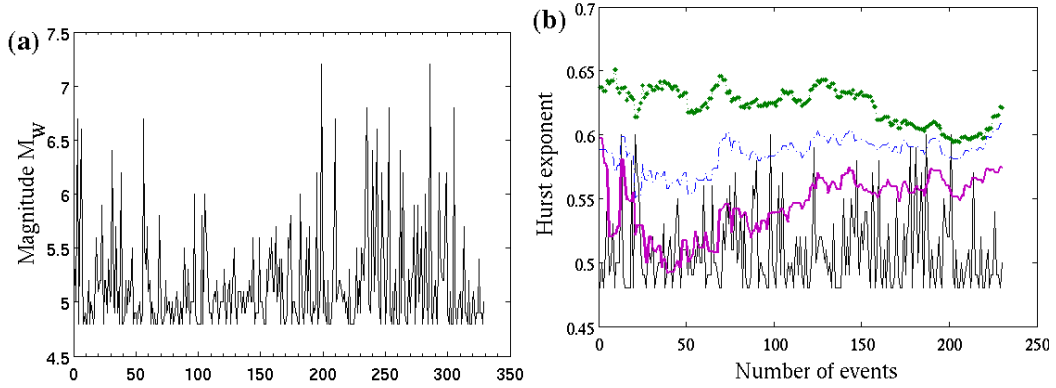


Figure 4: **(a)** Magnitude over the time from 0 to 350 events for the subduction zone. **(b)** Comparison between the magnitude of seismic events divided by a factor of 10 and the Hurst exponent calculated for the time series of interevent intervals for range defined from 100 to 330 events. Hurst exponents for three different minimum number of windows  $s_{min}$  are shown: upper equal to 2, middle equal to 4 and lower equal to 7.